Evaluation of Rule-Based Approaches for the Incorporation of Skeletal Muscle Fiber Orientation in Patient-Specific Anatomies

DUJ Keller, O Dössel, G Seemann

Institute of Biomedical Engineering, Karlsruhe Institute of Technology (KIT), Karlsruhe, Germany

Abstract

Skeletal muscle fiber orientation is important for the realistic calculation of body surface ECGs. However if computer models of patient-specific anatomies are created, usually no information about the muscle fiber arrangement is available. In this work we evaluated a published rule based approach to describe skeletal muscle fiber orientation together with two new methods. The quality of the respective fiber orientation approximation was assessed by comparing the forward calculated body surface potential maps (BSPMs) with the BSPM that was derived from a gold standard. Although all three methods showed comparable results the complete omission of skeletal muscle fiber orientation enhanced the BSPM even further. Thus it can be concluded that the characterization of skeletal muscle fiber orientation using a simplified approach is not feasible. In cases where no detailed information about the skeletal muscle fiber arrangement is available, it is better to entirely neglect its anisotropic influence.

1. Introduction

Skeletal muscle anisotropy is important for the realistic solution of the forward problem of electrocardiography. Whenever computer models of patient-specific anatomies are created usually no information about the muscle fiber arrangement in the heart or skeletal muscle is available. As in-vivo imaging techniques that can determine fiber orientation like Diffusion Tensor MRI are time-consuming and susceptible to motion artifacts, cardiac fiber orientation is frequently described using simplified rules [1, 2]. However, for the skeletal muscle there are only few suggestions for the implementation of fiber orientation into patient-specific models. Bradley et al. used a magnetic measurement device to track the skeletal muscle fiber directions of an anatomical dummy [3]. These fiber directions were then matched onto the torso model by a coordinate transformation that relied on previously determined anatomical landmarks. In contrast to this laborious and highly sophisticated approach which relies on the fidelity of the anatomical dummy, Klepfer et al. proposed a simplified, rule-based method. They considered the torso to be a cylinder around which the muscle fibers wrap. According to that, the torso is divided into twelve segments (from a cross-section perspective) and the fiber direction was assumed to be perpendicular to the bisector of each segment [4]. Finally Sachse et al. extracted the skeletal muscle fiber orientation from the highly detailed thin-section photos of the Visible Man dataset (National Library of Medicine, Bethesda, Maryland, USA) [5]. Automatic methods such as texture analysis and a 3D Sobel filter were used to derive an initial orientation which was then manually revised by human experts. In this work we evaluated the rule-based approach from Klepfer et al. together with two newly developed methods which were based on Klepfer's assumptions. The quality of the respective fiber orientation approximation was assessed by comparing the forward calculated body surface potential maps (BSPMs) with the BSPM resulting from the reference skeletal muscle fiber distribution developed by Sachse et al. for the Visible Man dataset.

2. Methods

As the reference fiber orientation was derived from the Visible Man dataset, it subsequently provided the anatomical basis for the simulation of the excitation conduction sequence as well as for the calculation of the body surface ECGs. The ten Tusscher model [6] was used to describe the electrophysiological characteristics of the ventricular tissue. To ensure a realistic repolarization sequence we included both transmural and apico-basal electrophysiological heterogeneities. I_{to} was modified in transmural direction as suggested by ten Tusscher et al. The ventricular walls were composed out of three distinct tissue layers (endocardium 40%, midmyocardium 40% and epicardium 20%) [7]. Changing tissue resistivity as well as transmural and apico-basal I_{Ks} heterogeneity was incorporated according to [8]. No electrophysiological differences between left and right ventricle were modeled. Ventricular activation was initiated using a special sequence of endocardial stimulation that imitates the role of the excitation conduction system [9]. Cardiac fiber orientation was incorporated into the ventricular model according to the measurements from Streeter [10]. The monodomain equations were used to simulate the current flow in the ventricular tissue. The electrophysiological model was pre-calculated in an uncoupled environment for a duration of 60s with a basic cycle length of 1s to tune gating variables and ionic concentrations.

The simulated transmembrane voltages were interpolated onto a finite element mesh of the ventricles and the BSPMs were calculated as described in [11]. The torso model comprised a total of 18 different tissues and fluids among which were: blood, lungs, liver, intestine, pancreas, spleen, kidneys, muscle (skeletal and heart), bones, cartilage and fat tissue. Anisotropic conductivity properties were considered for heart and skeletal muscle. The anisotropy factor (along:across) was set to 3:1. Tissue conductivities were assigned according to Gabriel et al. [12]. The body surface potentials were extracted at 64 positions (see figure 1) in order to calculate the RMS between the gold standard skeletal muscle fiber distribution [5] and the various rule-based approaches. The basic assumption of all rule-based approaches was that the skeletal muscle fibers are alligned parallel to the torso surface. Furthermore, most rule-based methods neglected the muscle fiber component that is oriented from head to feet (longitudinal orientation). The following fiber orientation datasets were considered in the evaluation:

- Klepfer: The fiber direction was assumed to be perpendicular to the bisector of the twelve segments in which the thorax was subdivided [4].
- Gradient: A 3D Sobel filter was used on the torso geometry filled with an increasing gray value from inside to outside which generated a vector that was normal to the thoracic surface in every voxel. Fiber orientation was assumed to be perpendicular to the plane formed by these normal vectors and the longitudinal torso orientation.
- Gold+No-Z: Realistic fiber orientation from the gold standard [5]. However, the longitudinal component of the fiber vectors was erased.
- Gradient+Back: Same as Gradient. Additionally, the back muscles which are known to be mainly longitudinally orientated were integrated accordingly.
- Only-Heart: No skeletal muscle anisotropy is considered (only cardiac fiber orientation data is taken into account).

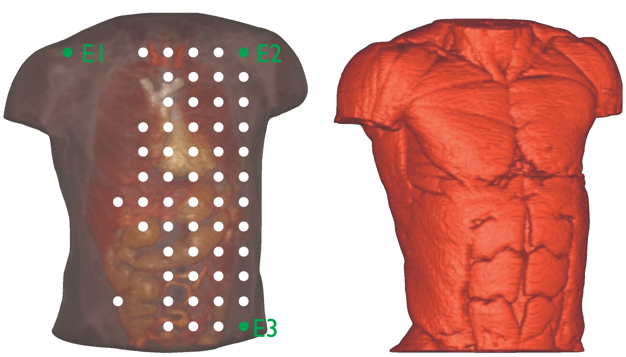

Figure 1. A: Transparent visualization of the highly detailed Visible Man torso with superimposed electrode positions (7 electrodes are located on the back). Einthoven 1: E2-E1; Einthoven 2: E3-E1. B: Skeletal muscle layer of the Visible Man torso.

3. Results

Figure 2 shows a visualization of the fiber orientation generated with the various approaches. The gold standard (figure 2 A) showed a much more complex fiber distribution than the simplified models (figure 2 B, C). Especially the abdominal region as well as the upper arms, neck and the back muscles displayed a strong longitudinal component. In contrast to that, the approach from Klefper et al. negelects all longitudinal orientations and showed discrete orientation transitions every 30° degrees as the method relied on the bisectors of the twelve cross-sectional segments (see arrows in figure 2 B). The gradient approach used in figure 2 C created a smoothened circumferential orientation. In this case the back muscles were additionally set to the longitudinal orientation (Gradient+Back).

The impact of the skeletal muscle fiber orientation on the standard Einthoven 1 and Einthoven 2 leads are shown in figure 3. In figure 3 A the ECG resulting from the gold standard fiber distribution is displayed which constitutes the reference. It is interesting to note, that the changes in the QRS complex strongly depend on the ECG lead (compare figure 3 B and C). Whereas the fiber orientation influence is evident in the Einthoven 1 lead, changes are much smaller in the Einthoven 2 lead. During the repolarization sequence (T Wave) changes are evident in both leads. However, in Einthoven 1 the simplified approaches underestimated the T Wave amplitude but overestimated its amplitude in Einthoven 2. Based on the two Einthoven leads, no coherent evaluation of the simplified methods could be made as two setups performed equally well:

Table 1. BSPM-RMS errors between the gold standard and the artificially generated fiber orientation setups.

Fiber orientation setup	RMS
Klepfer	8.8e-5
Gradient	8.9e-5
Gold+No-Z	8.3e-5
Gradient+Back	5.5e-5
Only-Heart	4.0e-5

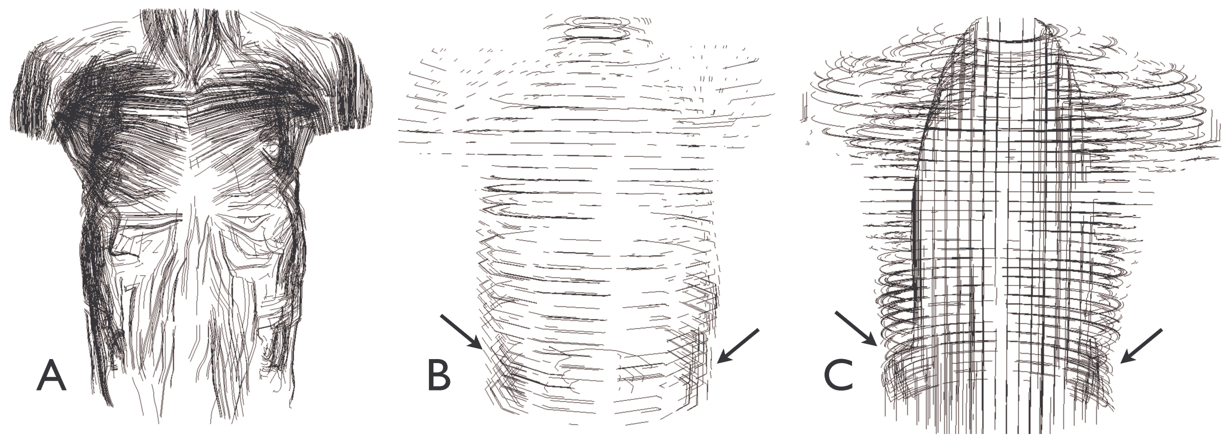

Figure 2. Fiber orientation visualization: the lines are constructed by following the fiber orientation starting from user-defined points. A: Complex fiber orientation of the gold standard (ventral view). Muscles in the abdominal area, upper arms, neck and back have a strong longitudinal component. B: Fiber orientation created using the Klepfer method from a ventral view (arrows denote visible orientation transitions). C: Fiber orientation created using the Gradient+Back approach (dorsal view / arrows denote smoothened orientation transitions).

- Gradient+Back: performed best with regard to QRS of Einthoven 1 and T Wave of Einthoven 2
- Only-Heart: performed best with regard to QRS of Einthoven 2 and T Wave of Einthoven 1

The changes of the BSPMs due to varying skeletal muscle orientation were evaluated by comparing the respective RMS values (see table 1). All approaches that neglected the longitudinal components showed similar RMS values (see Klepfer and Gradient). A comparable error is introduced if the longitudinal component of the gold standard setup is set to zero (Gold+No-Z). The incorporation of longitudinally alligned back muscles improves the RMS significantly (see Gradient+Back). However, if the skeletal muscle fiber orientation is neglected entirely, the RMS is even further enhanced (see Only-Heart).

4. Discussion and conclusions

Although skeletal muscle fiber orientation is known to be important for the calculation of BSPMs reliable data is rarely available. Because of this, most studies are based on fiber orientation setups that are generated following simplified rules. In this work, we compared these rule-based approaches with a highly detailed gold standard in order to evaluate their usability for patient-specific models of the thorax where normally no detailed knowledge of the fiber arrangement is available. All simplified approaches (except Gradient+Back) neglected the longitudinal components of the fiber orientation. This resulted in an underestimation of the signal amplitudes in the Einthoven 1 lead as well as in an overestimation of the Einthoven 2 amplitudes. This effect is attributed to the projected direction of the respective lead configuration in conjunction with the simplified fiber arrangement. As longitudinal components are ignored, the fibers of the simplified approaches lie parallel to the Einthoven 1 lead. The larger conductivity along the muscle fibers led to a broadening of the BSPM peaks in fiber direction. Thereby the signals at the two Einthoven 1 electrodes became more similar which reduced the lead's signal amplitude. In case of the Einthoven 2 lead, the absence of a longitudinal fiber component led to a constriction of the BSPM peaks and thus to an increase in signal amplitude. RMS comparison showed that all simplified approaches performed worse than a setup where the skeletal muscle fiber orientation was completely omitted. This is due to the omission of the longitudinal components. Adding the longitudinally oriented back muscles (Gradient+Back) at least partially enhanced the results. The close resemblance of the simplified approaches and the gold standard without longitudinal orientation (Gold+No-Z) however shows that the assumption of the circumferential orientation is valid and that there is no significant inclination of the muscle fibers towards the torso's interior. The presented results depend on the anisotropy ratio that was used (3:1). There are reports of much higher skeletal muscle anisotropy ratios in the literature (up to 15.3:1, compare [13]). Lead-depend changes are expected to increase with higher anisotropy ratios thereby probably also increasing RMS differences. It should therefore be noted, that a simplistic approach to include the skeletal muscle anisotropy as used in [4] or [14] can induce large errors in the calculation of the BSPM. In cases where no detailed information about the skeletal muscle fiber arrangement is available, it is better to entirely neglect its anisotropic influence.

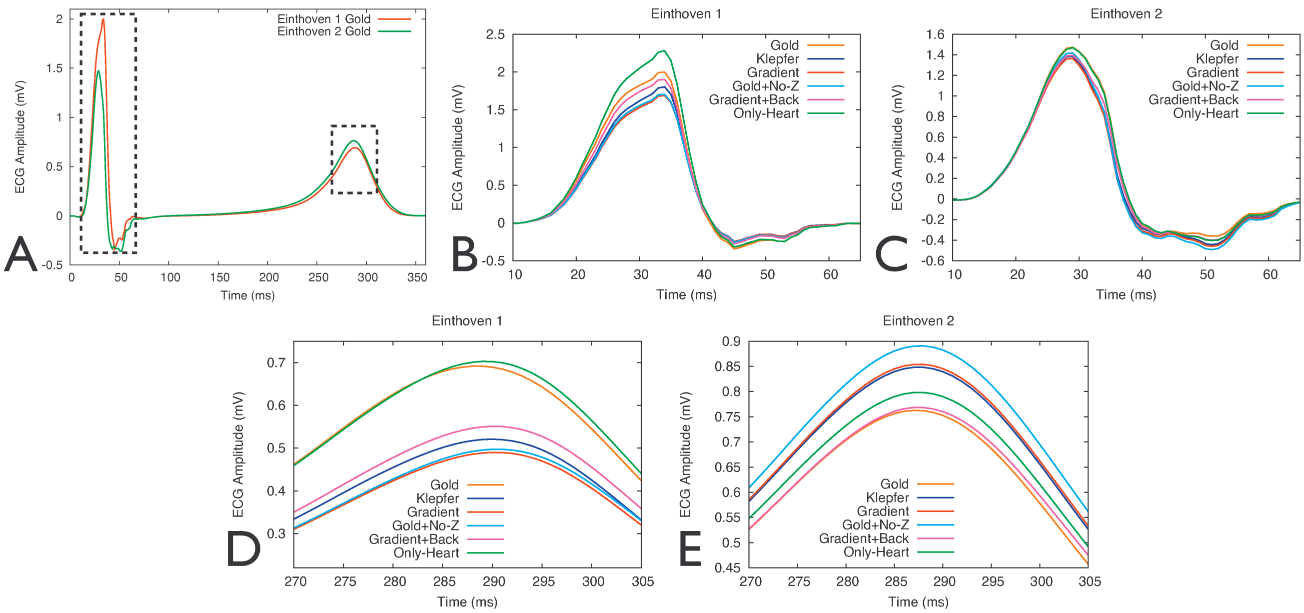

Figure 3. A: Simulated Einthoven 1 and 2 lead based on the gold standard fiber orientation. Designated areas are enlarged in B,C and D,E respectively. B and C show the influence of the skeletal muscle fiber orientation on the QRS complex. D and E visualizes the changing amplitudes during the T Wave.

References

[1] Nielsen P, LeGrice I, Hunter P, Smaill B. Mathematical model of geometry and fibrous structure of the heart. Am J Physiol 1991;260:H1365–H1378.

[2] Potse M, Dubé B, Richter J, Vinet A, Gulrajani R. A comparison of monodomain and bidomain reaction-diffusion models for action potential propagation in the human heart. IEEE Trans Biomed Eng 2006;53:2425–2435.

[3] Bradley C, Pullan A, Hunter P. Effects of material properties and geometry on electrocardiographic forward simulations. Annals of Biomedical Engineering 2000;28:721–741.

[4] Klepfer R, Johnson C, MacLeod R. The effects of inhomogeneities and anisotropies on electrocardiographic fields: A 3-d finite-element study. IEEE Transactions on Biomedical Engineering 1997;44:706–719.

[5] Sachse F, Wolf M, Werner C, Meyer-Waarden K. Extension of anatomical models of the human body: Three dimensional interpolation of muscle fiber orientation based on restrictions. Journal of Computing and Information Technology 1998;6:95–101.

[6] ten Tusscher K, Noble D, Noble P, Panfilov A. A model for human ventricular tissue. American Journal of Physiology Heart and Circulatory Physiology 2004;286:H1573–89.

[7] Sicouri S, Antzelevitch C. Distribution of m cells in the canine ventricle. J Cardiovasc Electrophysiol 1994;5:824–837.

[8] Keller D, Kalayciyan R, Dössel O, Seemann G. Fast creation of endocardial stimulation profiles for the realistic simulation of body surface ecgs. In IFMBE Proceedings WC. 2009; accepted.

[9] Kalayciyan R, Keller D, Seemann G, Dössel O. Creation of a realistic endocardial stimulation profile for the visible man dataset. In IFMBE Proceedings WC. 2009; accepted.

[10] Streeter D. Handbook of Physiology: The Cardiovascular System, volume I. American Physiology Society, 1979; 61–112.

[11] Farina D. Forward and Inverse Problems of Electrocardiography: Clinical Investigations, volume 4 of Karlsruhe Transactions on Biomedical Engineering. Karlsruhe: Universitätsverlag Karlsruhe, 2008; .

[12] Gabriel S, Lau R, Gabriel C. The dielectric properties of biological tissues: III. parametric models for the dielectric spectrum of tissues. Physics in Medicine and Biology 1996; 41:2271–2293.

[13] Rush S, Abildskov J, McFee R. Resistivity of body tissues at low frequencies. Circ Res 1963;12:40–50.

[14] Karlon W, Lehr J, Eisenberg S. Finite element models of thoracic conductive anatomy: sensitivity to changes in inhomogeneity and anisotropy. IEEE Transactions on Biomedical Engineering 1994;41:1010–1017.

Address for correspondence:

David UJ Keller
Institute of Biomed. Eng. Karlsruhe Insititute of Technology
Kaiserstrasse 12, 76131 Karlsruhe, Germany
David.Keller@Kit.Edu